TISSUE ENGINEERING: Part A
Volume 29, Numbers 13 and 14, 2023

DOI: 10.1089/ten.tea.2022.0223

ORIGINAL ARTICLE

Small-Caliber Vascular Grafts Engineered from Decellularized Leaves and Cross-Linked Gelatin

Nicole Gorbenko, Gianna Rinaldi, Amalia Sanchez, and Nick Merna, PhD

Despite advances in vascular replacement and repair, fabricating small-diameter vascular grafts with low thrombogenicity and appropriate tissue mechanics remains a challenge. A wide range of platforms have been developed to use plant-derived scaffolds for various applications. Unlike animal tissue, plants are primarily composed of cellulose which can offer a promising, nonthrombogenic alternative capable of promoting cell attachment and redirecting blood flow. By taking advantage of the biocompatibility and mechanical properties of cellulose, we developed small-diameter vascular grafts using decellularized leatherleaf viburnum and cross-linked gelatin. Different terrestrial plant leaves (leatherleaf, spinach, and parsley) were decellularized with sodium dodecyl sulfate, egtazic acid and/or Tergitol, followed by a bleach and Triton X-100 clearing solution, and then evaluated for decellularization efficiency, mechanical integrity, and recellularization potential. Hematoxylin and eosin staining and DNA quantification revealed successful removal of cells in all leatherleaf conditions. Methods of 3D graft fabrication were evaluated, and leatherleaf scaffolds maintained suitable tensile and rupture strength properties. 2D scaffolds and 3D grafts were seeded with rat endothelial cells. Cells remained viable for over 14 days with cell densities comparable to other natural and synthetic scaffolds. This study demonstrates the potential of cost effective and readily available decellularized plants to generate small-diameter vascular grafts capable of recellularization and with suitable mechanical properties.

Keywords: decellularization, vascular graft, plant, small-diameter, sodium dodecyl sulfate, endothelial cell

Impact Statement

Due to the prevalence of coronary heart disease in the United States, small-caliber vascular grafts for coronary bypass surgery are in high demand. We evaluate decellularized plant leaves as potential candidates for small-diameter vascular grafts with appropriate mechanical properties and recellularization potential.

Introduction

Coronary artery disease accounts for 610,000 (one in four) deaths annually in the United States.[1] Surgical intervention involves arterial bypass to redirect blood flow around blocked arteries. As a result, there is a growing need for synthetic, natural, and hybrid polymer small-diameter vascular graft alternatives to autologous vessels. Attempts have been made to enhance endothelialization and minimize thrombosis in synthetic grafts using extracellular matrix proteins and growth factors.[2,3] It is also necessary to match mechanical properties of native vessel and graft material, to prevent suture-line stress concentrations.[4,5]

Structural similarities between animal and plant tissues inspired a recent strategy of decellularizing plants for patches and 3D scaffolds for vascular, skeletal, bone, and

Bioengineering Program, Fred DeMatteis School of Engineering and Applied Science, Hofstra University, Hempstead, New York, USA.

cardiac tissue engineering.[6–10] Plant cell walls contain cellulose, embedded with pectin and lignin.[11,12] Plant-derived cellulose is accessible, inexpensive, and biocompatible, with tunable mechanical properties. Gelatin cross-linked with glutaraldehyde has been extensively studied for medical applications; examples include vascular sealant in surgery and tissue adhesive for reinforcing acutely dissected aortic wall.[13–16] The aim of this study was to construct robust and endothelialized small-diameter vascular grafts using decellularized plant leaves with cross-linked gelatin.

Studies utilizing sodium dodecyl sulfate (SDS) and Triton X-100 with plants present promising and cost effective pathways for cell removal, compared to protocols using DNase or supercritical carbon dioxide.[17,18] However, decellularization efficacy of Tergitol and egtazic acid (EGTA) has not been tested on plants. We previously demonstrated that decellularization potentially damages the structure and mechanical properties of umbilical cord arteries.[19] Preservation of extracellular matrix structure during decellularization is crucial to prevent immediate distension of vascular grafts upon implantation.[20] In this study we investigate structural and mechanical changes in plant extracellular matrix resulting from different decellularization protocols.

A successful tissue engineered vascular graft requires an appropriate combination of scaffold, cell source, and cell seeding strategy to maintain long-term patency and minimize thrombosis *in vivo*. We engineered vessels with suitable mechanical properties using plant-derived scaffold and cross-linked gelatin. We hypothesize that surface roughness and small pore size of decellularized leatherleaf will enhance recellularization of endothelial cells (ECs) and better recapitulate the lumen of native vessels.

Materials and Methods

Plant leaf decellularization

Fresh leatherleaf viburnum, spinach, and parsley were rinsed in deionized water and decellularized through one of four pathways in an orbital shaker at 37°C (Fig. 1):

(1) *SDS*: 72 h in 2% SDS (Sigma-Aldrich) in deionized water refreshed every 24 h.
(2) *SDS/EGTA*: alternating between 24 h in 2% SDS and 24 h in 0.05% EGTA in deionized water (Sigma-Aldrich) for 96 h.
(3) *Tergitol/EGTA*: alternating between 24 h in 1% Tergitol in deionized water (Sigma-Aldrich) and 24 h in 0.05% EGTA for 96 h.
(4) *Tergitol/SDS*: alternating between 24 h in 1% Tergitol and 24 h in 2% SDS for 96 h.

Pathways were followed with 6 h in clearing solution (10% bleach and 0.1% Triton X-100 in deionized water), sterilization in 70% ethanol for 1 h, and storage in PBS for up to 1 week at 4°C.

DNA quantification

Thirty to fifty milligram of intact (nondecellularized) and decellularized plant leaf was ground (Kimble Pellet Pestle), weighed, and digested with lysis buffer containing proteinase K (Omega Bio-Tek) for 30 min at 56°C. DNA was extracted using magnetic beads and measured photometrically at 260 nm.

Tensile testing

Decellularized plant leaves and glutaraldehyde cross-linked gelatin sheets (control) were cut into dog-bone shapes (Fig. 2C). Digital calipers measured gauge length, thickness, and width of each sample's narrowest section. Samples were pulled uniaxially at 0.08 mm/s until failure (Fig. 2D). True strain, true stress, maximum tensile stress, and elastic modulus were calculated from measured load and extension.

Maximum modulus, tensile stress, and failure stain of 3D grafts were analyzed as previously described.[21,22] Grafts were mounted between two steel pins, prestretched for three cycles to 10% strain, then pulled until failure at 0.08 mm/s.

Histological staining

Intact and decellularized leatherleaf fixed in 4% formaldehyde (Sigma-Aldrich) for 1 h, stored in ethanol, was sent to VitroVivo Biotech (Rockville, Maryland) for paraffin embedding and hematoxylin and eosin (H&E) staining. Additional samples were stained in-house with 1% Safranin O or 1% Toluidine Blue. Brightfield microscopy was performed at 10×, 20×, and 40× magnification (BioTek).

Scanning electron microscopy

A 10×10 mm intact, SDS-, SDS/EGTA-, Tergitol/EGTA-, and Tergitol/SDS-decellularized leatherleaf, spinach, and

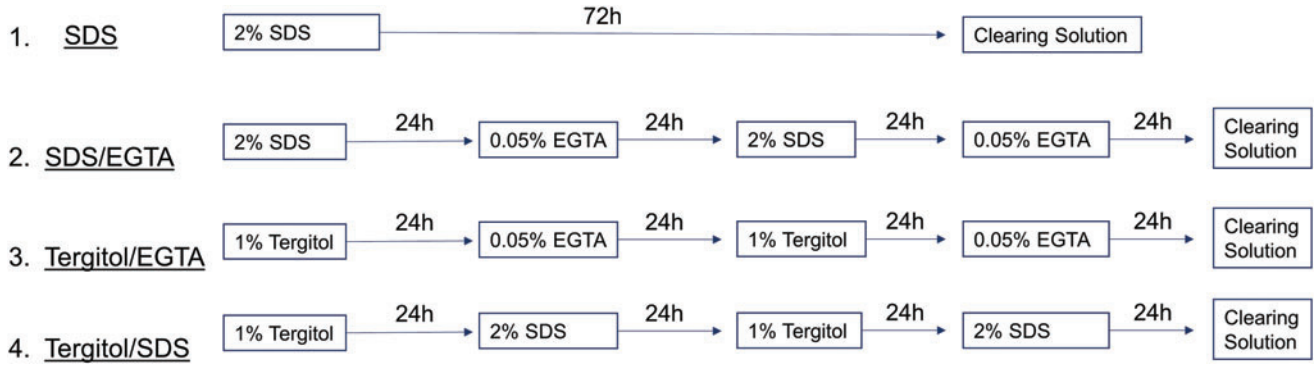

FIG. 1. SDS (1), SDS/EGTA (2), Tergitol/EGTA (3), and Tergitol/SDS (4) decellularization followed by a 6 h treatment with clearing solution. EGTA, egtazic acid; SDS, sodium dodecyl sulfate. Color images are available online.

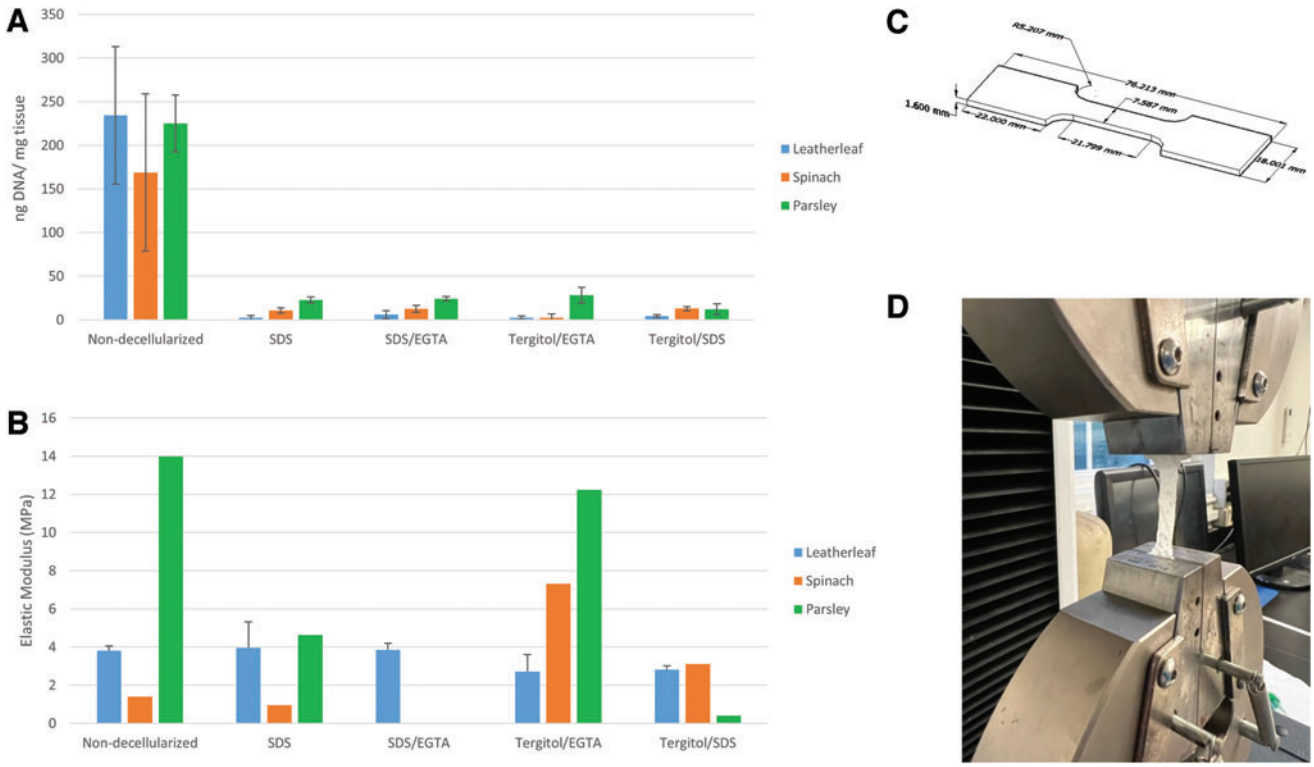

FIG. 2. DNA content **(A)** and Elastic Modulus **(B)** for intact, SDS-, SDS/EGTA-, Tergitol/EGTA-, and Tergitol/SDS-decellularized leatherleaf, spinach, and parsley. A custom printed stencil **(C)** was used to cut samples into a dog-bone shape for tensile testing **(D)**. Color images are available online.

parsley were fixed and rinsed with ascending ethanol concentrations (70–100%) for 1 h. Samples were dried in a Samdri-795 critical point dryer (Tousimis), mounted on aluminum stubs, and coated with gold using an EMS-550 sputter coater. A Quanta FEI-250 scanning electron microscope (SEM) imaged abaxial and adaxial surfaces of leatherleaf, spinach, and parsley with and without cell seeding at 200× and 800× magnification. Pores were measured manually at 800×.

Fabrication of 3D grafts

SDS- and SDS/EGTA-decellularized leatherleaf, spinach, and parsley cut to 25×42 mm were wrapped once around an acrylic rod 2 mm in diameter, using the adaxial side as the inner surface. A measure of 88.2 µL of 30%, 40%, 50%, or 60% gelatin heated to 55°C, mixed with 11.76 µL of 25% glutaraldehyde (Sigma-Aldrich), was applied evenly along the leaf's width (Supplementary Fig. S1). Remaining leaf was wrapped around the rod, held for 1 min to allow gelatin to cross-link, and incubated at 37°C overnight. Additional grafts were constructed with fibrin using 50 µL of 70 mg/mL fibrinogen (Sigma-Aldrich) with 50 µL of 20 U/mL thrombin (Sigma-Aldrich). Tubes created as a control using 50% gelatin and 25% glutaraldehyde had identical dimensions to 3D decellularized leatherleaf grafts.

Assessment of graft thickness and diameter

3D SDS-decellularized leatherleaf grafts were submerged in polydimethylsiloxane at 10:1 parts base to curing agent. Polydimethylsiloxane was cured for 1 h at 72°C. Grafts were sectioned into seven equal segments. Thickness and inner diameter of each segment were recorded.

Burst pressure testing

3D grafts (leatherleaf, spinach, parsley) and gelatin tubes were secured to barb adapters using parafilm. One end was attached to a pressure sensor (Automation Products Group, Logan, UT). A syringe was used to inject water into the other end at constant pressure. A slow-motion camera recorded peak pressure before failure. Leatherleaf grafts stored in cell growth medium were assessed at day 1, 7, 30, 60, or 90.

2D seeding: recellularization of plant leaves

Cell culture. Primary rat aortic ECs from Cell Applications (San Diego, CA), expanded in Heracell 150i CO_2 incubators (Thermo Scientific) with 5% CO_2, were used up to passage seven. Cells were fed with Rat EC Growth Medium (Cell Applications) supplemented with 2% fetal calf serum, endothelial growth supplement, epidermal growth factor, basic fibroblast growth factor, heparin, and hydrocortisone.

2D seeding. Decellularized leaves were coated with 20 µg/mL fibronectin (Sigma-Aldrich) for 1 h. Select conditions remained uncoated. ECs seeded at 625,000/cm^2 were incubated for 2 h before feeding. As a control, ECs were seeded onto cross-linked gelatin with and without fibronectin at 625,000/cm^2. After 5 days, recellularized samples were rinsed in PBS, fixed in 4% formaldehyde, and stained with diamidino-2-phenylindole (DAPI) nuclear stain for 5 min.

Blinded counters manually recorded nuclei in three confluent regions on each sheet ($n=9$) using fluorescence microscopy (Zeiss Axio Vert.A1) at 5×. Additional samples were trypsinized, and cells were counted 2, 24, or 48 h after seeding.

Scratch assays were performed on ECs in fibronectin coated six well plates using 1000 μL pipette tips. In one well, 50% gelatin and 25% glutaraldehyde were mixed. Images taken immediately after scratches and 24 h later were used to measure gap distances in ImageJ and determine cell migration rate.

Recellularization of 3D grafts

Acellular 3D grafts were filled with fibronectin (20 μg/mL) with barb adapters attached at both ends and incubated for 1 h. A measure of 1.5×10^6 ECs/mL was injected into each graft until capacity. Seeded grafts were incubated at 37°C in cell culture media and rotated 90° every 15 min for 3 h. Cells were gravity fed for 5 days, then evaluated using DAPI staining and imaging as previously described. Remaining samples were trypsinized to count adhered cells.

Statistical analysis

Anderson–Darling tests determined if data were normally distributed, and two-tailed Student's paired *t*-tests determined statistical significance (p-value <0.05) through Microsoft Excel. Data are expressed as mean ± standard deviation. All sample sizes ($n=3$) describe biological replicates unless stated otherwise.

Results

Assessment of decellularization

Decellularized leatherleaf was opaque, whitish, and rough. Decellularization reduced leatherleaf thickness from 0.4 ± 0.03 to 0.32 ± 0.05 mm ($p=0.04$). Decellularized spinach and parsley were smooth and translucent (Fig. 3), and thickness decreased from 0.7 ± 0.22 to 0.06 ± 0.01 ($p=0.02$) and 0.34 ± 0.15 to 0.17 ± 0.05 mm ($p=0.09$), respectively. All decellularized leaves were less stiff than intact samples, except for spinach treated with Tergitol (Fig. 2B). DNA quantification (Fig. 2A), histology (Fig. 4A), and DAPI staining (Fig. 4B) confirmed cell removal. DNA content (ng/mg tissue) was 234.3 ± 78.9, 2.3 ± 2.6, 5.9 ± 4.6, 2.5 ± 1.9, and 4.1 ± 1.7 for intact, SDS-, SDS/EGTA-, Tergitol/EGTA-, and Tergitol/SDS-decellularized leatherleaf, respectively. Decellularization removed over 97% ($p=0.018$), 92% ($p=0.08$), and 87% ($p<0.01$) of DNA for leatherleaf, spinach, and parsley, respectively. Residual DNA in leatherleaf (<50 ng DNA/mg tissue) represented satisfactory DNA removal.

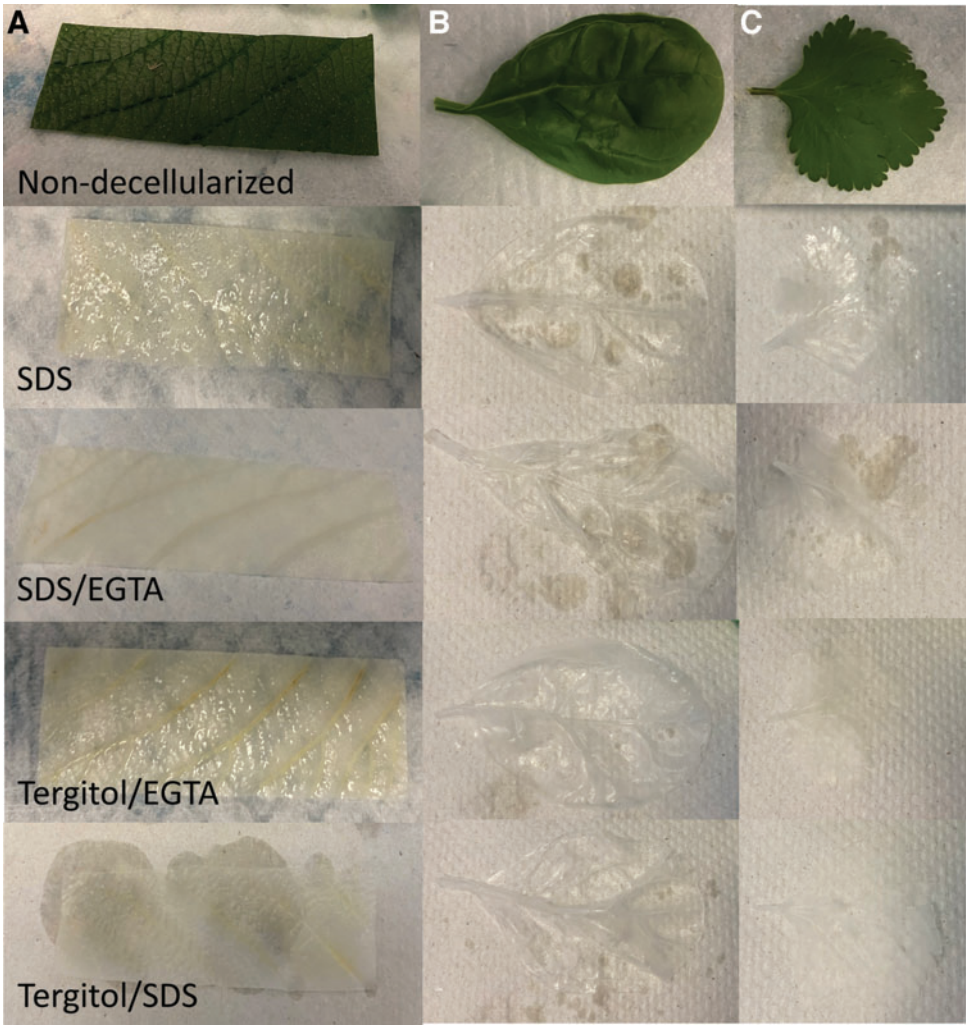

FIG. 3. Representative images of intact, SDS-, SDS/EGTA-, Tergitol/EGTA-, and Tergitol/SDS-decellularized leatherleaf viburnum **(A)**, spinach **(B)**, and parsley **(C)**. Color images are available online.

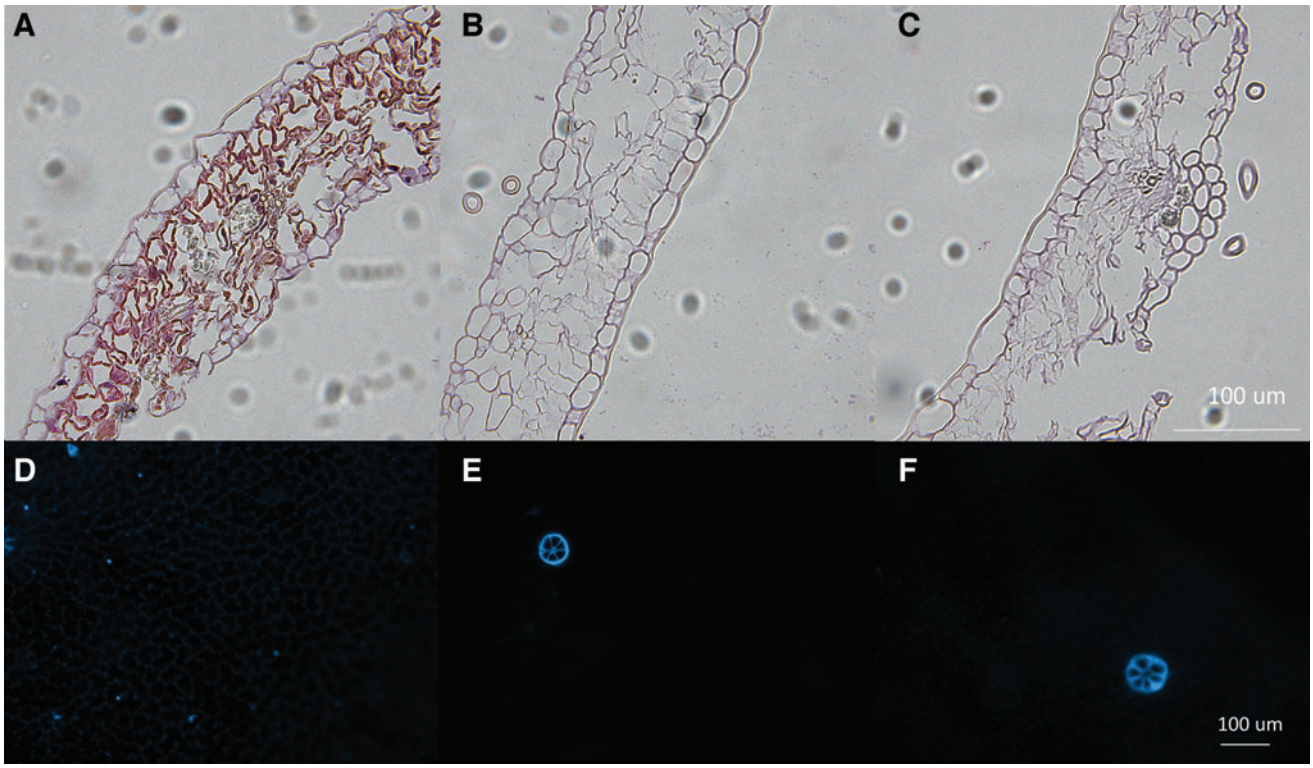

FIG. 4. Representative H&E staining for visualization of structure of intact **(A)** and SDS- **(B)** and SDS/EGTA-decellularized **(C)** leatherleaf cross-section at 40× magnification. Representative images of DAPI nuclear counterstain on the adaxial surface of leatherleaf before **(D)** and after decellularization with SDS **(E)** and SDS/EGTA **(F)**. DAPI, diamidino-2-phenylindole; H&E, hematoxylin and eosin. Color images are available online.

Elastic modulus was 3.8 ± 0.2, 4.0 ± 1.4, 3.9 ± 0.3, 2.7 ± 0.9, and 2.8 ± 0.2 MPa for intact, SDS-, SDS/EGTA-, Tergitol/EGTA-, and Tergitol/SDS-decellularized leatherleaf, respectively. Tergitol/SDS-decellularization reduced elastic modulus of leatherleaf (by 26%, $p < 0.01$), unlike other decellularization conditions. Elastic modulus of spinach was 1.15 ± 0.22, 1.62 ± 0.58, 0.54 ± 0.77, 4.05 ± 1.33, and 2.34 ± 1.09 MPa for intact, SDS-, SDS/EGTA-, Tergitol/EGTA-, and Tergitol/SDS-decellularization, respectively. Parsley was 4.47 ± 0.16, 3.59 ± 1.47, 2.28 ± 0.62, 1.21 ± 0.17, and 0.21 ± 0.29 MPa, respectively. Elastic modulus of cross-linked gelatin was 0.3 ± 0.1 MPa, and failure strain was 0.1 ± 0.02.

Leatherleaf microstructures were qualitatively evaluated through SEM imaging and histology. Intact leaves had an upper and lower epidermis containing mesophyll and vascular bundles (Fig. 4A). Decellularization with SDS and SDS/EGTA (Fig. 4B, C) removed all cellular components from the cellulose structure as confirmed with DAPI staining (Fig. 4D–F). Pores remained visible after decellularization. Safranin O staining revealed red lignified cell walls in leatherleaf that remained after decellularization with SDS and SDS/EGTA (Supplementary Fig. S2). Chromosomes and cell nuclei stained dark red were removed. Toluidine staining showed greenish-blue xylem that was not visible after decellularization. However, parenchyma and cell walls stained dark purple were conserved.

SEM imaging revealed multibranched trichomes on abaxial surfaces of leatherleaf before and after all decellularization conditions (Fig. 5), giving a fuzzy texture. Decellularization had no effect on trichome density, but Tergitol and EGTA damaged them. Spinach and parsley had no trichomes. Leatherleaf, spinach, and parsley contained pores evenly distributed over abaxial surfaces of each leaf (Fig. 6). SDS/EGTA decreased leatherleaf pore size from 15.8 ± 2.2 to 12.9 ± 1.2 μm ($p < 0.001$), but SDS had no effect. SDS and SDS/EGTA decreased parsley pore size from 19.8 ± 3.0 to 15 ± 1.8 ($p = 0.001$) and 15.7 ± 1.0 μm ($p = 0.001$), respectively. Spinach pores increased after SDS and SDS/EGTA-decellularization, from 14 ± 1.2 to 18.4 ± 1.1 ($p < 0.001$) and to 17.5 ± 1.4 μm ($p = 0.001$), respectively (Supplementary Fig. S3). Tightly packed cell walls on adaxial surfaces remained after decellularization, providing a smooth texture.

Assessment of 3D grafts

Burst pressure testing. Burst pressures of 3D grafts were 18.1 ± 14.8, 11.0 ± 8.2, 17.0 ± 7.9, and 12.1 ± 5.0 psi for decellularized leatherleaf with 30%, 40%, 50%, or 60% gelatin and 25% glutaraldehyde (Fig. 7). Burst pressures of 3D grafts constructed from decellularized spinach or parsley combined with 50% gelatin were lower compared with leatherleaf grafts, with values of 0.1 ± 0.1 ($p < 0.05$) and 0.3 ± 0.3 psi ($p < 0.05$), respectively. Pure cross-linked gelatin tubes had burst pressure of 2 ± 1.4 psi, 88% lower compared with leatherleaf grafts ($p < 0.05$). Increasing concentrations of gelatin decreased cross-linking times (between 5–20 s). Additional leatherleaf grafts were incubated in media at 37°C for up to 90 days. Burst pressures were 17.1 ± 7.9, 13.7 ± 4.3, 13.1 ± 2.5, 13.4 ± 3.9, and 13.9 ± 1.9 psi at day 1, 7, 30, 60, and 90, respectively. No changes

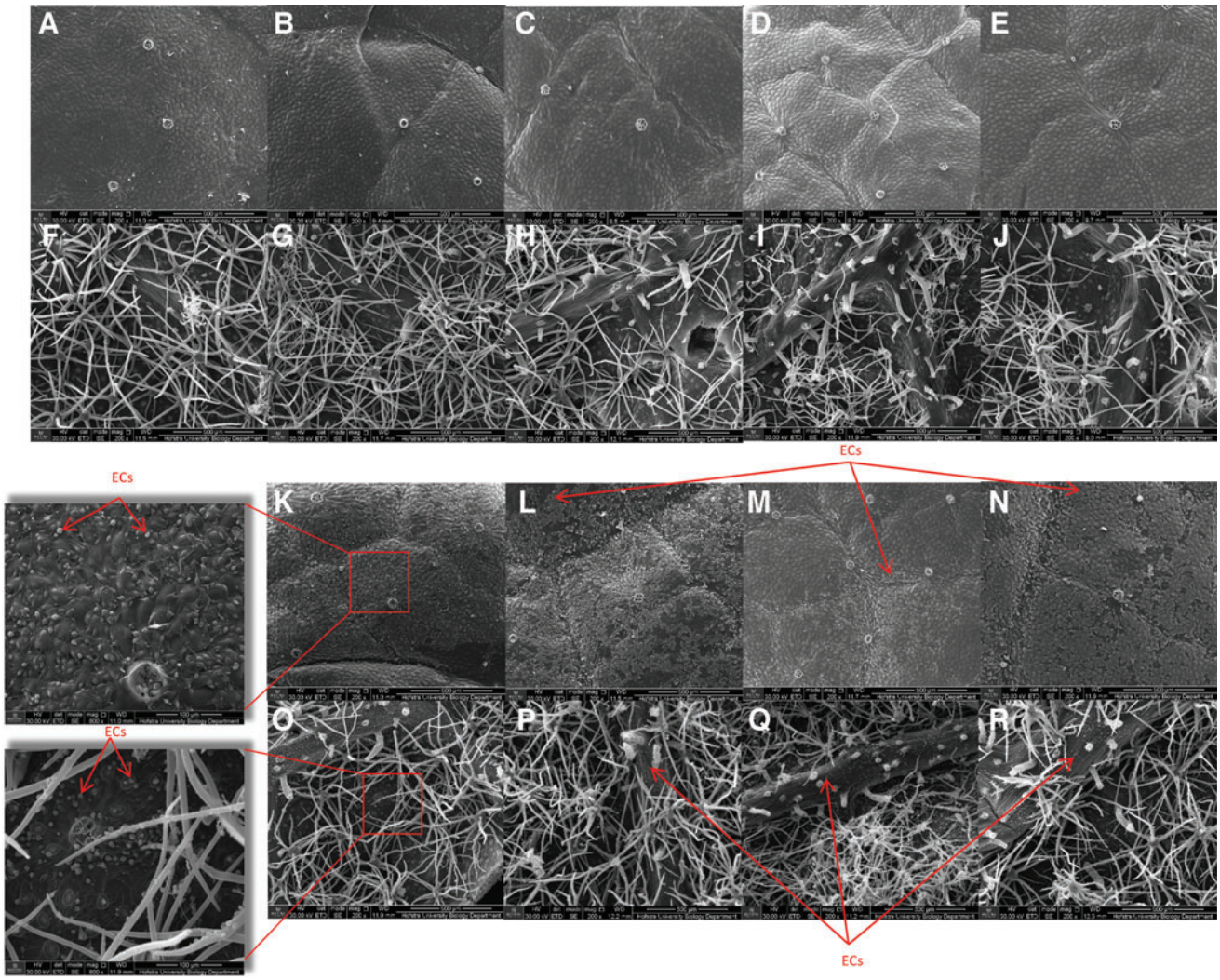

FIG. 5. Representative 200× magnification SEM images of the adaxial and abaxial surfaces of leatherleaf before **(A, F)** and after decellularization with SDS **(B, G)**, SDS/EGTA **(C, H)**, Tergitol/EGTA **(D, I)**, Tergitol/SDS **(E, J)**. Representative images of leatherleaf seeded with ECs (K–R). ECs are indicated by *red arrows* on the abaxial and adaxial surfaces with 800× magnification. ECs, endothelial cells; SEM, scanning electron microscope. Color images are available online.

in burst pressure occurred over time ($p > 0.2$). SDS-decellularized 3D grafts containing fibrin measured burst pressures below 0.1 psi.

Measurement of graft dimensions. Average wall thickness for leatherleaf grafts was $1.09 \pm .05$ mm with no difference in thickness along the length of each graft ($p > 0.21$) or between grafts ($p > 0.17$). Average inner diameter was $2.08 \pm .05$ mm, and no difference was observed along the length of each graft ($p > 0.19$) or between grafts ($p > 0.39$).

Tensile testing. Maximum modulus of 3D grafts constructed from SDS-decellularized leatherleaf and gelatin was 1.3 ± 0.1 MPa. Maximum tensile stress at failure was 5.5 ± 1.1 MPa, and failure strain was 4.1 ± 0.7.

Recellularization of 2D sheets

Decellularized leatherleaf coated with fibronectin was seeded with ECs to assess recellularization potential. Cells adhered within 2 h and increased in number by 19.8% ($p = 0.03$) and 55.7% ($p < 0.01$) after 24 and 48 h when trypsinized and counted (Fig. 8H). Rate of proliferation was lower compared with ECs cultured on polystyrene. SDS- and SDS/EDTA-decellularized leatherleaf seeded with ECs and stained with DAPI after 5 days (Fig. 8A, B) had 1296 and 1450 cells/mm^2, respectively. Adhered cells were distributed unevenly when seeded on uncoated leatherleaf. While SDS-decellularized leatherleaf without fibronectin reduced cell density by 62% ($p < 0.05$), cells adhered successfully to uncoated SDS/EGTA-decellularized leatherleaf ($p > 0.05$) (Fig. 8). Compared to leatherleaf, cells seeded onto pure cross-linked gelatin had lower densities of 633 and 817 cells/mm^2 ($p < 0.05$) with and without fibronectin coatings, respectively (Fig. 8C, F).

To evaluate effects of trichomes on cell seeding, both sides of leatherleaf samples were coated with fibronectin and seeded with ECs. SEM revealed cell adhesion to adaxial surfaces of SDS-, SDS/EGTA-, and Tergitol/SDS-decellularized leatherleaf (Fig. 5K–N), but lower cell

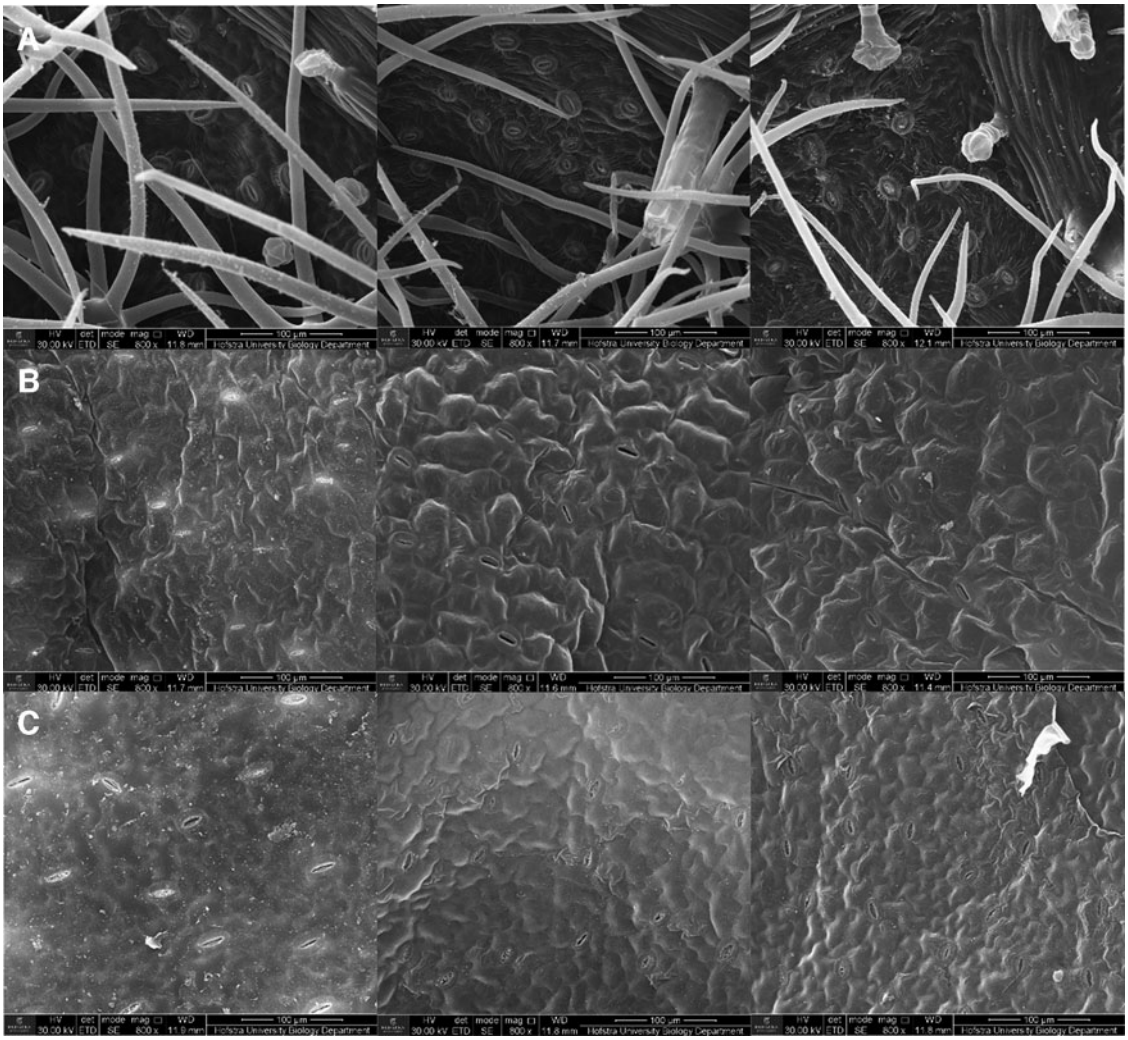

FIG. 6. Representative SEM images at 800× magnification illustrating pores present on the abaxial surface of leatherleaf **(A)**, spinach **(B)**, and parsley **(C)** before decellularization, after decellularization with SDS, and after decellularization with SDS/EGTA.

densities on abaxial surfaces (containing trichomes) for all conditions (Fig. 5O–R). Cross-linked gelatin reduced EC migration rate by 73% ($p < 0.01$) in scratch assays (Fig. 8I), compared to untreated controls.

Recellularization of 3D grafts

3D grafts fabricated using SDS- or SDS/EGTA-decellularized leatherleaf, 50% gelatin, and glutaraldehyde were recellularized with ECs. DAPI staining revealed cell adhesion to the lumen, and no gelatin was present on these surfaces (Fig. 9A). Manual counting of cell nuclei by DAPI staining showed similar cell densities at day 5 for SDS- and SDS/EGTA-decellularized leatherleaf (1174 vs. 1192 cells/mm^2, $p = 0.06$). Evaluation of cell density by trypsinization at day 7 resulted in values of 840 cells/mm^2 for both conditions. By day 14, cell density on SDS-decellularized leatherleaf increased to 1157 cells/mm^2, compared to 1847 cells/mm^2 for SDS/EGTA-decellularized leaves (Fig. 9B). H&E staining confirmed cell adhesion to decellularized leatherleaf sheets and 3D grafts (Fig. 9C, D).

Discussion

Small-caliber engineered blood vessels should exhibit suitable tensile and rupture strength properties, with a luminal surface to reduce blood coagulation and maintain patency.[23] While decellularized plants are being extensively studied for tissue engineering, we present a novel method for generation of small-caliber vascular grafts using plant-derived scaffolds and cross-linked gelatin. SDS, EGTA, bleach, and Triton X-100 removed DNA from leatherleaf, while preserving mechanical properties of extracellular matrix. Combining decellularized leatherleaf with cross-linked gelatin improved mechanical properties and endothelialization, compared to cross-linked gelatin alone.

DNA removal in decellularized leatherleaf was confirmed by DNA quantification and H&E and DAPI staining, with comparable results to other studies.[7,8] Pores were visible after decellularization with and without DAPI staining due to autofluorescence generated at those wavelengths.[24,25] Incomplete DNA removal and reduced mechanical properties in decellularized spinach and parsley were primary factors in choosing leatherleaf for subsequent cell seeding

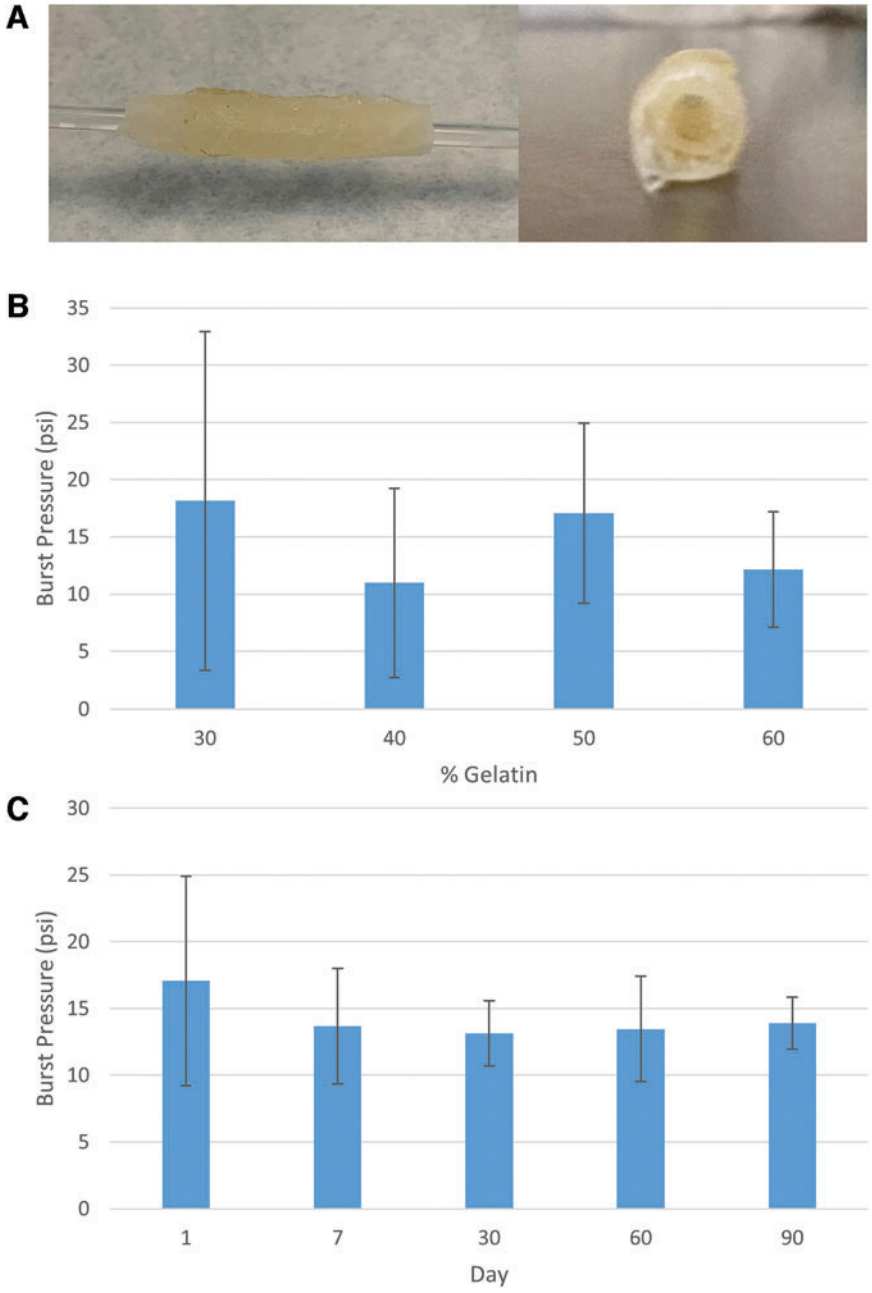

FIG. 7. Representative images of graft generated with SDS-decellularized leatherleaf **(A)**. Burst pressure values at day 1 for grafts fabricated using 30%, 40%, 50%, or 60% gelatin **(B)**. Burst pressure values at days 1, 7, 30, 60, and 90 for grafts fabricated using 50% gelatin **(C)**. Color images are available online.

experiments. Leatherleaf is larger, enabling more applications than spinach and parsley.

SEM revealed multibranched trichomes and pores on abaxial surfaces of leatherleaf, which increased water absorption. Conversely, smooth adaxial surfaces had reduced water absorption. Decellularization had no discernible effect on these structures. Previous SEM imaging of SDS-decellularized spinach reveals no topographical changes on its surface;[7] however, trichome damage was reported for decellularized olive leaves.[26] This was paired with higher cytotoxicity and reduced elastic modulus, possibly due to increased time in clearing solution and shorter water rinses, compared to our protocol. This highlights the importance of clearing solution and water rinse timing during decellularization.

SDS- and SDS/EGTA-decellularization with an orbital shaker had little effect on mechanical properties of leatherleaf, while Tergitol-decellularization reduced elastic modulus. Therefore, SDS- and SDS/EGTA-decellularization were chosen for subsequent experiments. Perfusion decellularization has been successful with spinach and parsley due to their vascular network, while soaking methods have been used for bulky structures such as apple and onion.[7,10] Clearing solution was essential for our decellularization, giving each leaf its translucent appearance as previously reported.[7,8] However, exposure to clearing solution exceeding 6 h led to decreased mechanical properties. Many protocols use clearing solutions to decellularize plant leaves for 24–48 h with higher concentrations of SDS, which reduces mechanical properties.[7,18]

In this study, deionized water rinsing was essential for removing residual detergents. Furthermore, prolonged exposure to ethanol during sterilization increased stiffness

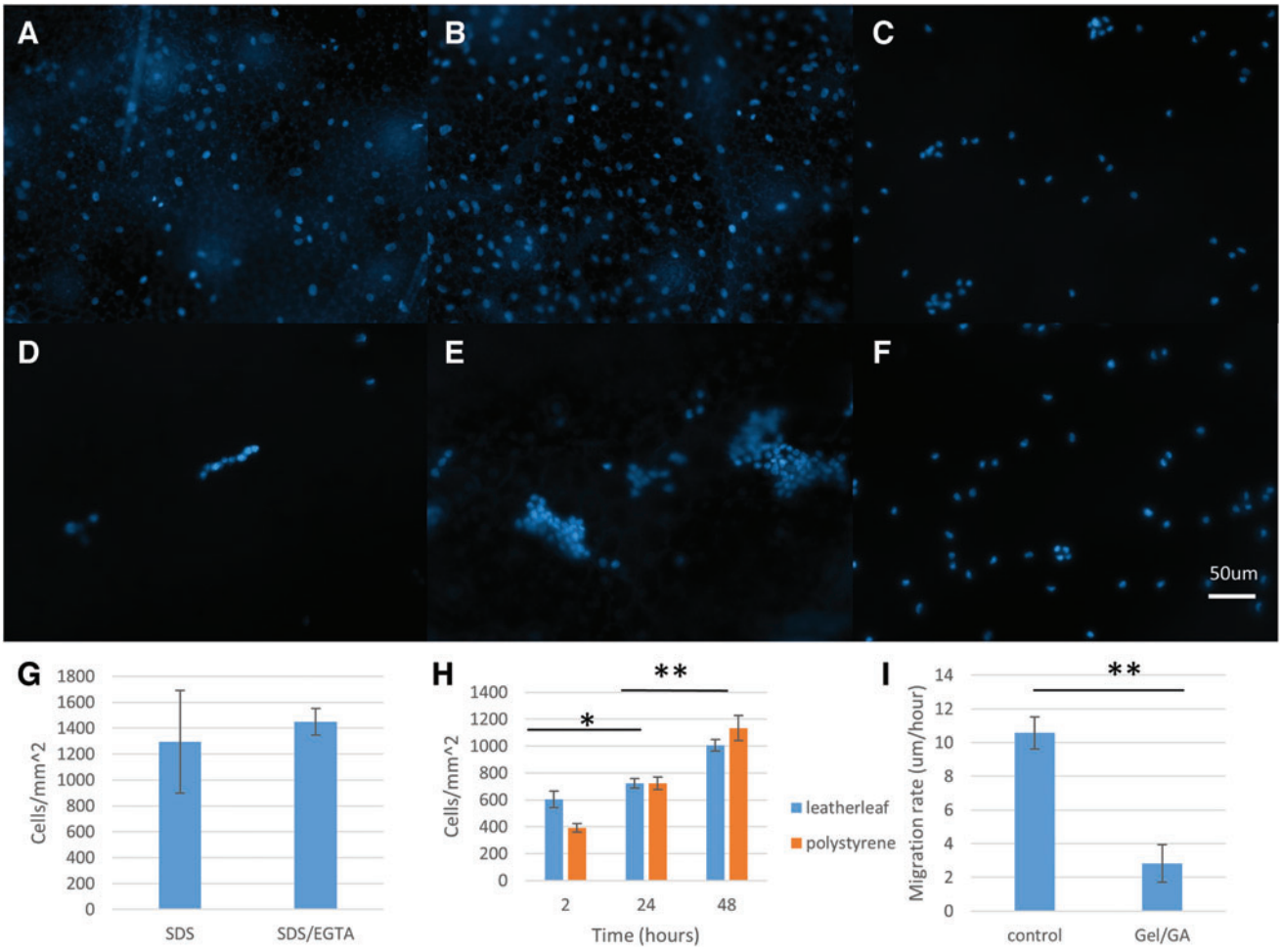

FIG. 8. Representative 10× magnification images of ECs seeded on SDS- **(A)** and SDS/EGTA-decellularized leatherleaf viburnum **(B)**, and cross-linked gelatin **(C)** with fibronectin coating and without fibronectin coating **(D–F)** and stained with DAPI nuclear counterstain. EC count from DAPI stained images **(G)** and by cell passaging **(H)**. Scratch assay for untreated and gelatin/glutaraldehyde coated ECs **(I)**. $*p<0.05$, $**p<0.01$ and error bars represent SD. SD, standard deviation. Color images are available online.

potentially due to molecular rearrangement as previously shown for silk and nanocomposite biomaterials.[27,28] Previously, SDS or clearing solution alone failed to decellularize spinach, indicating that both anionic and nonionic detergents may be needed.[7] Supercritical carbon dioxide was reported to remove DNA from spinach quickly, but it reduced ultimate tensile strength compared to chemical treatments.[29] Decellularizing plant root with DNAase removed DNA in 30 min,[30] but it costs more than SDS ($410/g tissue vs. $3/g). Cost and mechanical properties will be important to consider when scaling up and commercializing these methods.

Standardized decellularization of plants is necessary for clinical testing and FDA approvals. Different growing conditions produced leatherleaf varying slightly in thickness and mechanical properties. Minor adjustments to decellularization times compensated for these differences, producing scaffolds with consistent DNA removal and mechanical properties. In addition, leatherleaf can be collected year-round during hot and cold months with similar decellularization quality. Variations in leatherleaf thickness before decellularization did not affect wall thickness of each 3D graft. Wall thickness and inner diameter remained uniform along the length of each graft which will help maintain even stress distribution under perfusion. Similar to ePTFE and Dacron, plant cellulose won't degrade *in vivo,* preventing debris formation which could cause adverse reactions.[31] However, studies show that cellulase or oxidizing agent sodium periodate can enhance cellulose degradation to promote regeneration *in vivo.*[32,33]

Maintenance of vascular graft integrity is essential to proper function upon implantation. 3D decellularized leatherleaf combined with cross-linked gelatin had a maximum modulus comparable to native vessel and other tissue engineered grafts, higher maximum tensile stress and failure strain, and maintained burst pressures for 90 days *in vitro.*[34] Others reported that glutaraldehyde cross-linked gelatin can provide good mechanical properties and thermal resistance with minimal cytotoxicity.[13,35] Thousands of bioprosthetic implants successfully utilized glutaraldehyde cross-linking clinically over the last two decades despite reports on its cytotoxicity.[36] Pure cross-linked gelatin exhibited higher elasticity, but lower maximum stress, failure strain, and burst pressure than our 2D and 3D decellularized plant grafts. Increasing gelatin concentration improved mechanical

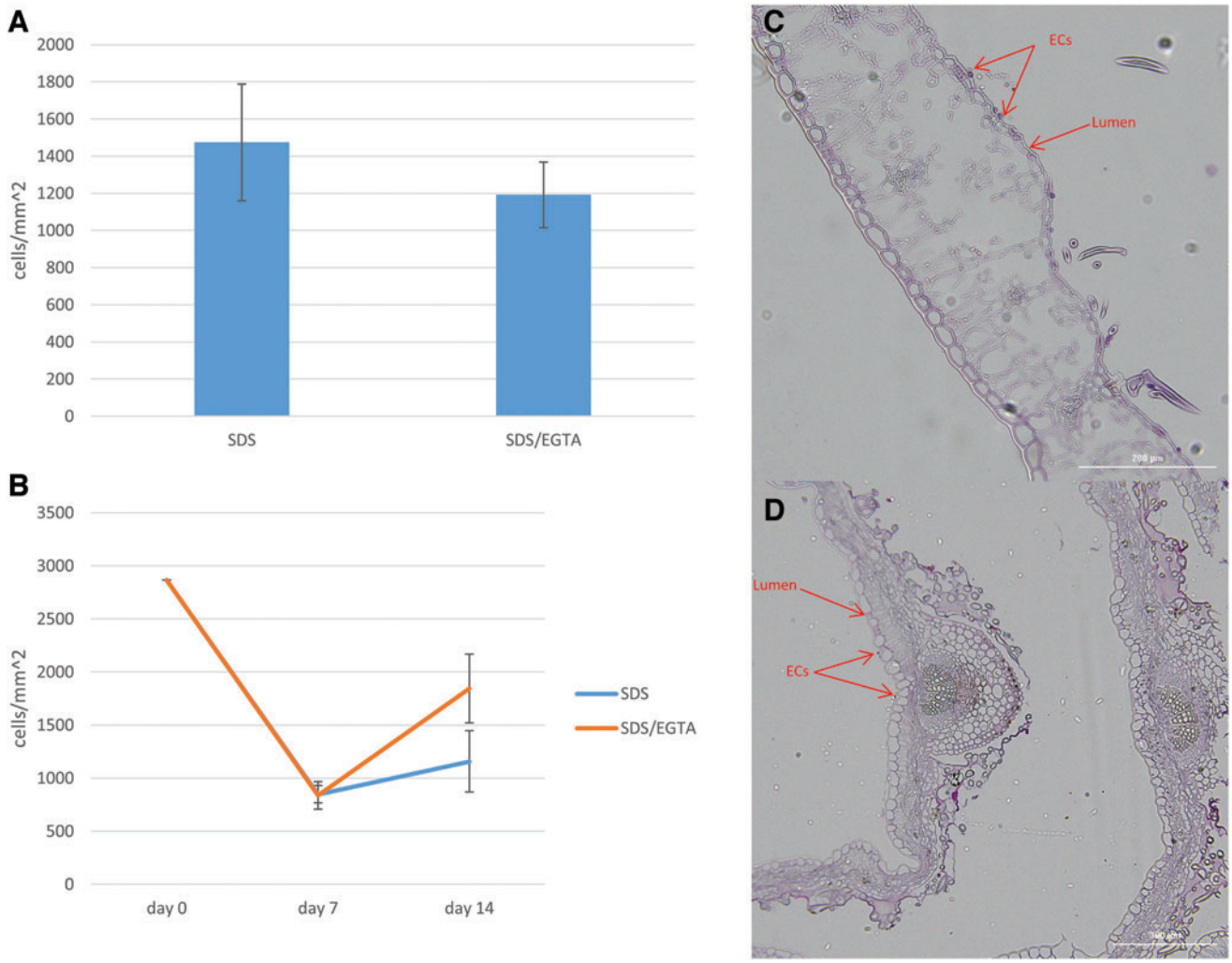

FIG. 9. EC count from DAPI stained images 5 days after seeding in 3D grafts **(A)** and by cell passaging 7 and 14 days after seeding **(B)**. Representative H&E staining for visualization of 2D **(C)** and 3D **(D)** seeding of ECs onto decellularized leatherleaf. Error bars represent SD. The *red arrows* indicate the ECs and the lumen. Error bars represent standard deviation. Color images are available online.

performance of 3D leatherleaf scaffolds but decreased cross-linking time.

Burst pressures were measured in 3D spinach/parsley grafts and gelatin tubes to better assess contributions of gelatin to overall mechanical strength of each graft. While gelatin was applied to each graft using identical methods, spinach/parsley grafts and gelatin tubes had lower burst pressures than 3D leatherleaf grafts. This suggests that decellularized leatherleaf and gelatin both contribute significantly to mechanical properties of our 3D grafts. Twenty-five percent glutaraldehyde increased mechanical strength and decreased cross-linking times, compared to 1% (data not shown). Combining gelatin with glutaraldehyde in our 3D scaffolds resulted in final glutaraldehyde concentrations of 3%, which was reported to provide an elastic modulus of 30 MPa with minimal cytotoxicity [13]. Reducing final concentrations of glutaraldehyde below 1% decreased mechanical properties. Fifty percent gelatin with 25% glutaraldehyde was selected for subsequent testing, as it possessed a balance between mechanical strength and cross-linking time.

Pat drying decellularized leaves before rolling were not necessary and reduced mechanical strength. This enables incubation of scaffolds in media with cells, before rolling 3D grafts, and incorporation of cells within inner layers in the future. Furthermore, a rod of any size can be used during the rolling process to generate vessels of desired diameter. We found that strength of cell-substrate bonds alone was unable to provide adequate burst pressures in plant-derived 3D grafts, which prompted initial testing of effects of cross-linked gelatin and fibrin on mechanical strength and cell seeding. 3D leatherleaf grafts using fibrin tissue adhesive did not sustain adequate mechanical properties. Overall, burst pressure and tensile strength of decellularized leatherleaf combined with cross-linked gelatin were comparable to other natural grafts.[20,37]

Before implantation, endothelialization of vascular scaffolds is necessary. ECs were successfully seeded on SDS- and SDS/EGTA-decellularized leatherleaf with and without fibronectin coating, resulting in similar viable cell densities after 5 days. Studies showed that fibronectin was preferred for decellularized plant tissues to mimic extracellular matrix

and promote EC attachment.[7,38,39] ECs seeded into vasculature of SDS-decellularized spinach remained viable 48 h after incubation.[7] Our cell densities were similar when evaluated by DAPI staining and cell passaging and comparable to densities reported for cardiomyocytes seeded onto decellularized spinach.[39] Studies reported stem cells and myoblasts adhering to decellularized Camellia japonica leaves, celery, and spinach without protein coatings or surface modifications.[40–42] We found that ECs adhered to decellularized leatherleaf without any coating, but less evenly compared to fibronectin coated leatherleaf.

Plant cells possess cell-matrix adhesion complexes similar to animal cells[43] and vitronectin-like proteins immunologically related to the substrate-adhesion molecule in several species of plants.[44] In addition, adhesive proteins are naturally found in fetal bovine serum. Atomic force microscopy previously revealed that decellularized spinach has appropriate surface roughness for trapping cells and high specific surface area to promote attachment.[42]

Our ECs adhered to adaxial surfaces at greater densities, compared to abaxial surfaces. Damage to trichomes resulting from Tergitol and EGTA had no visible effect on trichome density or cell adhesion. Adaxial surfaces of leatherleaf are likely more conducive to endothelialization because they provide a smoother surface. While both surfaces are suitable for cell attachment, the adaxial surface was more appropriate for endothelialization, as it achieved a more complete monolayer. For this reason, the adaxial side was chosen as the inner surface of our 3D grafts.

ECs proliferated rapidly within 48 h after seeding on SDS-decellularized leatherleaf, although slower than when cultured on polystyrene. Others reported reduced rate of cell proliferation on decellularized plant leaves, compared to stiff substrates.[38,39] Our cell density and rate of cell migration were lower on cross-linked gelatin, compared to decellularized leatherleaf, which could pose challenges when incorporating smooth muscle cells into inner layers in future studies. Others reported reduced rate of migration for tumor cells cultured on glutaraldehyde cross-linked gelatin micropatterns.[45]

Pore size and distribution are important for cell adhesion and migration. Before and after decellularization, pores on leatherleaf, spinach, and parsley (15–20 μm) were comparable to previous reports for parsley and vanilla.[12] These structures control gas and water exchange in plants and are larger in sweet pepper, carrot, and apple (250–800 μm).[12] While larger pores ranging from 200 to 250 μm are suitable for cell infiltration,[46] small pore size presents no problem for endothelializing engineered blood vessels.[47] Ideal pore size was reported to be 10–45 μm to support endothelial coverage and reduce fibrous tissue infiltration. ECs were unable to bridge pores exceeding cell-sized diameters.[48]

In summary, we constructed mechanically stable vascular grafts capable of recellularization using detergent-decellularized plant leaves and cross-linked gelatin. Cellulose is a desirable material for vascular grafts due to its mechanical strength, flexibility, blood compatibility, and small pore size. We adequately removed plant DNA, while maintaining tensile strength of these scaffolds. Our 3D grafts possessed uniform wall thickness, suitable burst pressure, and tensile strength. Subcutaneously implanted decellularized apple previously demonstrated mild immune response that disappeared after 8 weeks.[6] In future studies, plant-derived grafts will be preconditioned with fluid shear stress *in vitro* and assessed for blood compatibility, patency, suture retention, and mechanical strength *in vivo*. Inflammatory response will be measured *in vitro* using transwell migration of macrophages or T cells. Complement activation can then be assessed by flow rate, time, and area *in vitro* as previously described.[49] We believe that our approach will provide new and exciting applications for decellularized plants in vascular replacement and repair.

Acknowledgments

The authors thank Jonah Khorrami for preparation and imaging of SEM samples, the Department of Biology at Hofstra University for use of their SEM, Allison Meer for assistance in microtome operation and staining, and Dr. Michael Dores for use of his BioTek microscope.

Authors' Contributions

N.G.: methodology, investigation, validation, writing—review and editing. G.R.: conceptualization, methodology, investigation, writing—review and editing. A.S.: methodology, investigation, validation, writing—review and editing. N.M.: conceptualization, methodology, investigation, formal analysis, validation, resources, writing—original draft, writing—review and editing, supervision, project administration, funding acquisition.

Disclaimer

The content is solely the responsibility of the authors and does not necessarily represent the official views of the National Institutes of Health.

Disclosure Statement

No competing financial interests exist.

Funding Information

Research reported here was supported by the National Institute of Biomedical Imaging And Bioengineering of the National Institutes of Health under Award Number R15EB033168.

Supplementary Material

Supplementary Figure S1
Supplementary Figure S2
Supplementary Figure S3

References

1. Tsao CW, Aday AW, Almarzooq ZI, et al. Heart disease and stroke statistics—2022 update: A report from the American Heart Association. Circulation 2022;145(8):e153–e639.
2. Lu A, Sipehia R. Antithrombotic and fibrinolytic system of human endothelial cells seeded on PTFE: The effects of surface modification of PTFE by ammonia plasma treatment and ECM protein coatings. Biomaterials 2001; 22(11):1439–1446; doi: 10.1016/s0142-9612(00)00302-1
3. Crombez M, Chevallier P, Gaudreault RC, et al. Improving arterial prosthesis neo-endothelialization: Application of a

proactive VEGF construct onto PTFE surfaces. Biomaterials 2005;26(35):7402–7409; doi: 10.1016/j.biomaterials.2005.05.051
4. Ballyk PD, Walsh C, Butany J, et al. Compliance mismatch may promote graft-artery intimal hyperplasia by altering suture-line stresses. J Biomech 1998;31(3):229–237.
5. Sarkar S, Salacinski HJ, Hamilton G, et al. The mechanical properties of infrainguinal vascular bypass grafts: Their role in influencing patency. Eur J Vasc Endovasc Surg 2006;31(6):627–636; doi: 10.1016/j.ejvs.2006.01.006
6. Modulevsky DJ, Cuerrier CM, Pelling AE. Biocompatibility of subcutaneously implanted plant-derived cellulose biomaterials. PLoS One 2016;11(6):e0157894.
7. Gershlak JR, Hernandez S, Fontana G, et al. Crossing kingdoms: Using decellularized plants as perfusable tissue engineering scaffolds. Biomaterials 2017;125:13–22.
8. Dikici S, Claeyssens F, MacNeil S. Decellularised baby spinach leaves and their potential use in tissue engineering applications: Studying and promoting neovascularisation. J Biomater Appl 2019;34(4):546–559.
9. Latour ML, Tarar M, Hickey RJ, et al. Plant-derived cellulose scaffolds for bone tissue engineering. BiorXiv 2020.
10. Cheng Y-W, Shiwarski DJ, Ball RL, et al. Engineering aligned skeletal muscle tissue using decellularized plant-derived scaffolds. ACS Biomater Sci Eng 2020;6(5):3046–3054.
11. Caffall KH, Mohnen D. The structure, function, and biosynthesis of plant cell wall pectic polysaccharides. Carbohydr Res 2009;344(14):1879–1900.
12. Zhu Y, Zhang Q, Wang S, et al. Current advances in the development of decellularized plant extracellular matrix. Front Bioeng Biotechnol 2021;9:650.
13. Bigi A, Cojazzi G, Panzavolta S, et al. Mechanical and thermal properties of gelatin films at different degrees of glutaraldehyde crosslinking. Biomaterials 2001;22(8):763–768.
14. Deiber JA, Ottone ML, Piaggio MV, et al. Characterization of cross-linked polyampholytic gelatin hydrogels through the rubber elasticity and thermodynamic swelling theories. Polymer 2009;50(25):6065–6075.
15. Suzuki S, Ikada Y. Sealing effects of cross-linked gelatin. J Biomater Appl 2013;27(7):801–810.
16. Albes JM, Krettek C, Hausen B, et al. Biophysical properties of the gelatin-resorcinformaldehyde/glutaraldehyde adhesive. Ann Thorac Surg 1993;56(4):910–915.
17. Wang Y, Dominko T, Weathers PJ. Using decellularized grafted leaves as tissue engineering scaffolds for mammalian cells. In Vitro Cell Dev Biol Plant 2020;56(6):765–774.
18. Fontana G, Gershlak J, Adamski M, et al. Biofunctionalized plants as diverse biomaterials for human cell culture. Adv Healthc Mater 2017;6(8):1601225.
19. Wong V, Gada S, Singh M, et al. Development of small-caliber vascular grafts using human umbilical artery: An evaluation of methods. Tissue Eng Part C Methods 2023;29(1):1–10; doi: 10.1089/ten.TEC.2022.0144
20. Gui L, Muto A, Chan SA, et al. Development of decellularized human umbilical arteries as small-diameter vascular grafts. Tissue Eng Part A 2009;15(9):2665–2676; doi: 10.1089/ten.TEA.2008.0526
21. Gwyther TA, Hu JZ, Christakis AG, et al. Engineered vascular tissue fabricated from aggregated smooth muscle cells. Cells Tissues Organs 2011;194(1):13–24.
22. Luo J, Qin L, Kural MH, et al. Vascular smooth muscle cells derived from inbred swine induced pluripotent stem cells for vascular tissue engineering. Biomaterials 2017;147:116–132.
23. Niklason LE, Lawson JH. Bioengineered human blood vessels. Science 2020;370(6513):eaaw8682.
24. Jauneau A, Cerutti A, Auriac M-C, et al. Anatomy of leaf apical hydathodes in four monocotyledon plants of economic and academic relevance. PLos One 2020;15(9):e0232566.
25. Fricker M, White N. Wavelength considerations in confocal microscopy of botanical specimens. J Microsc 1992;166(1):29–42.
26. Ahangar Salehani A, Rabbani M, Biazar E, et al. The effect of chemical detergents on the decellularization process of olive leaves for tissue engineering applications. Eng Rep 2023;5(2):e12560.
27. Hofmann S, Stok KS, Kohler T, et al. Effect of sterilization on structural and material properties of 3-D silk fibroin scaffolds. Acta Biomater 2014;10(1):308–317.
28. Ahmed M, Punshon G, Darbyshire A, et al. Effects of sterilization treatments on bulk and surface properties of nanocomposite biomaterials. J Biomed Mater Res Part B Appl Biomater 2013;101(7):1182–1190.
29. Harris AF, Lacombe J, Liyanage S, et al. Supercritical carbon dioxide decellularization of plant material to generate 3D biocompatible scaffolds. Sci Rep 2021;11(1):1–13.
30. Phan NV, Wright T, Rahman MM, et al. In vitro biocompatibility of decellularized cultured plant cell-derived matrices. ACS Biomater Sci Eng 2020;6(2):822–832.
31. Wang D, Xu Y, Li Q, et al. Artificial small-diameter blood vessels: Materials, fabrication, surface modification, mechanical properties, and bioactive functionalities. J Mater Chem B 2020;8(9):1801–1822.
32. Kram HB, Nugent P, Reuben BI, et al. Fibrin glue sealing of polytetrafluoroethylene vascular graft anastomoses: Comparison with oxidized cellulose. J Vasc Surg 1988;8(5):563–568.
33. Mohan CC, Unnikrishnan P, Krishnan AG, et al. Decellularization and oxidation process of bamboo stem enhance biodegradation and osteogenic differentiation. Mater Sci Eng C 2021;119:111500.
34. Luo J, Qin L, Zhao L, et al. Tissue-engineered vascular grafts with advanced mechanical strength from human iPSCs. Cell Stem Cell 2020;26(2):251.e8–261.e8.
35. Zhan J, Morsi Y, Ei-Hamshary H, et al. In vitro evaluation of electrospun gelatin–glutaraldehyde nanofibers. Front Mater Sci 2016;10(1):90–100.
36. Jayakrishnan A, Jameela S. Glutaraldehyde as a fixative in bioprostheses and drug delivery matrices. Biomaterials 1996;17(5):471–484.
37. Tuan-Mu H-Y, Yu C-H, Hu J-J. On the decellularization of fresh or frozen human umbilical arteries: Implications for small-diameter tissue engineered vascular grafts. Ann Biomed Eng 2014;42(6):1305–1318.
38. Lacombe J, Harris AF, Zenhausern R, et al. Plant-based scaffolds modify cellular response to drug and radiation exposure compared to standard cell culture models. Front Bioeng Biotechnol 2020;8:932.
39. Robbins ER, Pins GD, Laflamme MA, et al. Creation of a contractile biomaterial from a decellularized spinach leaf without ECM protein coating: An in vitro study. J Biomed Mater Res Part A 2020;108(10):2123–2132.

40. Varhama K, Oda H, Shima A, et al. Decellularized plant leaves for 3D cell culturing. IEEE; 2019.
41. Campuzano S, Mogilever NB, Pelling AE. Decellularized plant-based scaffolds for guided alignment of myoblast cells. BioRxiv 2020.
42. Salehi A, Mobarhan MA, Mohammadi J, et al. Efficient mineralization and osteogenic gene overexpression of mesenchymal stem cells on decellularized spinach leaf scaffold. Gene 2020;757:144852.
43. Zhu JK, Shi J, Singh U, et al. Enrichment of vitronectin-and fibronectin-like proteins in NaCl-adapted plant cells and evidence for their involvement in plasma membrane–cell wall adhesion. Plant J 1993;3(5):637–646.
44. Seymour GB, Tucker G, Leach LA. Cell adhesion molecules in plants and animals. Biotechnol Genet Eng Rev 2004;21(1):123–132.
45. Han H-C, Liu Y-W, Chen C-Y. Attachment of tumor cells to the micropatterns of glutaraldehyde (GA)-crosslinked gelatin. Sens Mater 2008;20(8):435–446.
46. Zhang Z, Wang Z, Liu S, et al. Pore size, tissue ingrowth, and endothelialization of small-diameter microporous polyurethane vascular prostheses. Biomaterials 2004;25(1): 177–187.
47. Ju YM, San Choi J, Atala A, et al. Bilayered scaffold for engineering cellularized blood vessels. Biomaterials 2010; 31(15):4313–4321.
48. Salem AK, Stevens R, Pearson R, et al. Interactions of 3T3 fibroblasts and endothelial cells with defined pore features. J Biomed Mater Res 2002;61(2):212–217.
49. Lamba N, Gaylor J, Courtney J, et al. Complement activation by cellulose: Investigation of the effects of time, area, flow rate, shear rate and temperature on C3a generation in vitro, using a parallel plate flow cell. J Mater Sci Mater Med 1998;9(7):409–414.

Address correspondence to:
Nick Merna, PhD
Bioengineering Program
Fred DeMatteis School of Engineering
and Applied Science
Hofstra University
110 Weed Hall
Hempstead, NY 11549
USA

E-mail: nicholas.j.merna@hofstra.edu

Received: December 21, 2022
Accepted: April 10, 2023
Online Publication Date: May 8, 2023